Al-Nahrain Journal for Engineering Sciences **NJES** 28(4)531-544, 2025
http://doi.org/10.29194/NJES.28040531

Influence of Environmental Fluctuations on Non-Diffracting Beams Used to Secure Data

Kamal H. Kadem[1*], Mohammed F. Mohammed[2]

Authors affiliations:
1*) Dept. of Laser and Optoelectronics Engineering, Al-Nahrain University, Baghdad, Iraq.
st.kamal.hussein.phd@ced.nahrainuniv.edu.iq

2) Dept. of Laser and Optoelectronics Engineering, Al-Nahrain University, Baghdad, Iraq.
mohammed.al-temimi@nahrainuniv.edu.iq

Paper History:

Received: 18th Dec. 2024

Revised: 7th Apr. 2025

Accepted: 19th Apr. 2025

Abstract

In this study, an optical communications system was simulated that secures data transmitted in free space and relies on optical beams with varying responses to atmospheric disturbances. Atmospheric turbulence was also modeled with high accuracy to simulate real-world conditions. The optical beams in the system were represented by non-diffracting beams and compared in two scenarios, data transmission using a traditional communications system and in the second scenario, the communications system relies on the optifusion method. This approach facilitated a comprehensive study and analysis of the transmission environment and optifusion method effectiveness and the identification of the best non-diffracting beam types for secure data transmission. Through the values of selected performance metrics for non-diffraction beams across different weather conditions and long propagation distances, the study demonstrated the reliability of the proposed simulation system and the effectiveness of the improvement method in data security. The final results also showed that the non-diffracting beams resist atmospheric turbulence strongly and effectively, proving their ability to provide safe, long-range optical communications.

Keywords: Free-Space, Optical Communication, Optifusion, Non-Diffracting Beams, Atmospheric Turbulence, Scintillation Index, Overlap, Strehl Ratio.

تأثير التقلبات البيئية على الحزم غير الحيودية المستخدمة لتأمين البيانات

كمال حسين كاظم ، محمد فوزي محمد

الخلاصة:

تحاكي هذه الدراسة نظام اتصالات بصري في الفضاء الحر يعتمد بتأمين البيانات المرسلة على الحزم الضوئية ذات الاستجابات المتفاوتة للاضطرابات الجوية. تمت نمذجة الاضطرابات الجوية بدقة عالية لمحاكاة ظروف العالم الحقيقي بشكل وثيق. تم توليد حزم غير حيودية واستخدامها لتمثيل الحزم الضوئية ومقارنتها في سيناريوهين، نقلها البيانات بطريقة التقليدية ونقل وحماية البيانات بطريقة optifusion. قد سهّل هذا النهج إجراء تحليل شامل لبيئة الإرسال وفعالية optifusion، وتحديد أنواع الحزم غير حيودية الأكثر ملاءمة لنقل البيانات بشكل آمن. من خلال تحليل قيم مقاييس الأداء الرئيسية للحزم غير حيودية المختارة عبر الظروف الجوية المختلفة ومسافات الانتشار الطويلة، أثبتت الدراسة موثوقية نظام المحاكاة وفعالية طريقة optifusion في تعزيز أمن البيانات. كما أظهرت النتائج أن الحزم غير حيودية تظهر مقاومة قوية للاضطرابات الجوية، مما يؤكد قدرتها على توفير اتصالات بصرية آمنة وطويلة المدى في الفضاء الحر.

1. Introduction

Free-space optical (FSO) communications is a cost-effective wireless technology that offers high data rates and rapid deployment, making it ideal for environments where physical cabling is impractical. FSO is suitable for fast and efficient data transfer over short, medium, and long distances, including remote and deprived areas [1]. The propagation of optical beams in free space relies on a direct line-of-sight (LOS) connection between transmitting and receiving systems, ensuring secure data spread. The ease and versatility of control and generation of different optical beams make FSO communications systems useful for various applications. The FSO's structure is simple and easy to integrate with various communications networks, including terrestrial, satellite, and mobile platforms, increasing its expansion and adaptability to modern communications needs [2].

NJES is an **open access Journal** with **ISSN 2521-9154** and **eISSN 2521-9162**

FSO communications are better than RF communications in transmitting more data in a secure, high-speed manner and are superior to fiber-optic communications in terms of ease of field installation, system simplicity, efficiency, and low cost, thus reducing the need for underground and underwater excavation for laying fiber optics and also reducing the need for complex and expensive infrastructure. It is also a power-efficient system, as it consumes a minimum of power per bit transmitted and supports full-duplex communication for data exchange. FSO communication systems are suitable for various network infrastructures, such as integrated, local, and extended [3].

The weaknesses of FSO communications are mostly due to the free space in which the optical beams propagate, as weather conditions such as (fog, rain, snow, etc.) affect the quality of the propagated optical beams and their efficiency in transmitting data. Physical obstacles such as birds or buildings and alignment errors resulting from minor seismic activities further disrupt the efficiency of FSO communications [3].

Free-space disturbances affect not only FSO communications but also several other areas such as light detection and ranging (LiDAR), remote sensing, and imaging. In the LiDAR technologies, the effect of weather conditions on mapping, environmental analysis, and other tasks appears [4]. The remote sensing systems operate from a very long distance, and therefore atmospheric disturbances affect the accuracy and reliability of these systems [5]. Imaging systems also face major challenges due to atmospheric effects [6]. Therefore, studying and analyzing the effect of atmospheric turbulence on optical beams helps improve the performance of optical systems in many fields.

Recently, with the demonstration that (shape, amplitude, phase, and coherence) of optical beams affect their quality and thus the performance of the optical system, modified Gaussian beams have emerged [7]. That are resistant to atmospheric effects and help improve the performance of optical systems, including FSO. These beams are called non-diffracting due to their resistance to deflection when propagating in free space [8]. Non-diffracting beams have unique properties and distinct shapes from conventional optical beams, making them an important choice for FSO communications. From these properties (diffraction-free, self-healing, self-acceleration, and self-imaging) with the possibility of adding orbital angular momentum (OAM) and carrying it by non-diffracting beams [9].

There are several methods for generating these beams, including spatial light modulators (SLMs). Which we relied on in this research due to their ease of use, effectiveness, and the quality of the non-diffracting beams they produce. The capabilities of SLMs make them a versatile tool in both laboratory and practical applications [9]. In this research, chose the (Bessel, Airy, Vortex) beams that are characterized by their unique shapes and properties, as they are not identical, and therefore their interaction with the carried data, the method of protection, and the effects of atmospheric disturbances will differ from beam to another. Therefore, we will compare the behavior of these three beams and evaluate their performance when propagating through free space and under the influence of various atmospheric disturbances while carrying data, once in the traditional method and in another method by hiding the data inside them using one of the protection methods.

In this study, the optifusion method was applied to three carefully selected non-diffracting beams to demonstrate the effectiveness of this method with different types of beams. Where the optifusion method relies on hiding data in part of the optical beams without affecting the shape, intensity, and characteristics of the beam [10]. By combining the non-diffracting beams with the optifusion method without one affecting the other and taking advantage of both together, we create a protected and efficient FSO communication system.

In this study, we first aim to investigate data hiding using an optifusion method within non-diffracting beams. The second goal is to create a realistic and effective medium for optical beams to travel through so that the results of non-diffracting beams match real-life conditions, making the suggested communication system useful and applicable in the real world.

The proposed optical communication system, incorporating the generation of non-diffracting beams, the optifusion method, a free-space carrier medium, atmospheric turbulence effects, and all figures presented in this paper, was simulated using MATLAB R2022b (version 9.13) By a large number of scripts.

The structure of the paper is organized as follows: section 2 comparing with recent literature, section 3 covers atmospheric turbulence modeling, while Section 4 focuses on non-diffracting beams after optifusion method. Section 5 presents the system simulation, section 6 provides the analysis of results, and finally, section 7 concludes with the conclusion.

2. Comparing with Recent Literature

The advantages and effectiveness of the proposed security method for FSO communication are evident when compared with the latest insurance methods in the literature. But, research in this domain remains limited due to several challenges such as the (high costs associated with secure communication systems, particularly those designed for protection, and the inherent complexity of developing novel protection mechanisms). Therefore, innovative security approaches are often introduced cautiously and are not always thoroughly explored or readily accessible for evaluation.

The literature in this field is scarce, and existing research does not closely align, as each proposed technique tends to be fundamentally different. And this difference arises from the urgent need for uniqueness in security strategies because the weakness or compromise of a particular method makes any similar approach vulnerable to hacking. Therefore, in FSO communications, the comparable or closely related security methods to the one proposed in this work are exceptionally rare.

In a modern study, an OFDM signal was placed in a Gaussian beam and then masked by an image, known as a cover image. This method results in a laser that carries an image concealing the OFDM signal. This method has good performance in BER and flexibility under different weather conditions, while weaknesses might involve potential vulnerability to advanced analysis techniques and increased computational complexity due to the cover image [11]. When comparing this method to our approach, we observe that both methods leverage the OFDM signal due to its advantageous properties, including the ability to increase the amount of transmittable data. From a security standpoint, our approach is significantly superior by not using a cover image and this vulnerability by not providing an environment or visual context for eavesdroppers to target and by using non-diffracting beams instead of Gaussian beams, leveraging their unique properties and distinctive shapes to increase security and efficiency for the FSO communication system.

The second a study involves hiding a low-power optical beam inside another high-power optical beam. This approach is to coaxially transmit the strong and weak beams carrying different orthogonal spatial modes within a modal basis set, e.g., OAM modes. Although the weak beam has much lower power than that of the strong beam and the beams are in the same frequency band and on the same polarization, the two beams can still be effectively demultiplexed with little inherent crosstalk at the intended receiver due to their spatial orthogonality. However, an eavesdropper may not readily identify the weak beam when simply analyzing the spatial intensity profile [12]. This method is similar to our method of using a type of structured light beam, but its drawbacks are complexity and cost. Our proposed method is less expensive and simpler because it does not require multiple laser sources or separate high and low power beams.

By comparing the security method adopted in this research with the methods in the literature, despite their scarcity, we find simplicity, low cost, and effectiveness in relying on a single laser source. Relying on OFDM technology also increases the amount of hidden data that can be transmitted while enhancing security through non-diffracting beams. Our use of non-diffracting beams also helps increase the propagation distance in free space due to their unique properties and shapes that help resist atmospheric disturbances and camouflage to increase the security of the system.

3. Atmospheric Turbulence Modeling

Atmospheric turbulence plays a critical role in FSO communications, significantly affecting optical beams and their propagation. This is due to random fluctuations in the atmospheric refractive index, caused by changes in temperature, pressure, and humidity, and that leads to (intensity scintillation, beam wander, angle of arrival variations, etc.), all of which negatively impact the stability and quality of the optical beam.

And there are several models for simulating free-space atmospheric turbulence, and the most famous is the Kolmogorov model. Which is fundamental, depicting turbulence as a cascade of energy from large to small eddy scales. There are other models, such as the Hufnagel - Valley (H-V) model, which is popular for altitude-specific turbulence. The Greenwood Frequency model uses wind speed profiles to estimate turbulence frequency. The Bufton Wind model also provides a practical approach for modeling wind speed with elevation changes [13]. These models are valuable tools for evaluating the quality of optical beams under different weather conditions, and despite their usefulness, most face limitations. Including homogeneity assumptions and challenges in accurately capturing complex turbulence effects.

The use of the Kolmogorov spectral model has spread widely to represent atmospheric turbulence, but it has shown several obstacles, the most important of which is the deviation of turbulence at high altitudes, thus deviating from Kolmogorov behavior and showing non-Kolmogorov behavior. Therefore, turbulence models that integrate Kolmogorov and non-Kolmogorov behavior have been developed to provide greater accuracy in representing atmospheric turbulence. These models account for the complex dynamics of atmospheric turbulence across different altitudes, offering a better understanding of optical beam propagation in various atmospheric layers [14].

Where the von Kármán model appeared, which is different from the Kolmogorov model in that it introduces outer and inner scales and small-scale energy dissipation, in addition, it limits the sizes of the eddies, and this enables it to fully capture the effects of turbulence. Thus, this approach generates accurate modeling that is useful for FSO communication systems, as it generates perturbations that affect optical coherence and stability of optical beams [15].

In this study, the von Kármán model is used because it improves the Kolmogorov spectrum by effectively modeling the dissipation range and offering a more comprehensive representation of atmospheric turbulence. The von Kármán model is precious for capturing large-scale disturbances and subtle fluctuations affecting long-range [16]. To provide realistic atmospheric turbulence, in this study we used random phase screens based on the von Kármán model, integrated into the SLM. This approach allows precise control of the turbulence parameters and enables us to create various atmospheric conditions that we need to study and examine optical beams and various FSO communication systems.

Since such turbulence disrupts the initial beam modes and thus the possibility of losing the data it carries, this calls for the construction of detailed models to represent refractive index differences [17]. In this section we will build the numerical model of atmospheric turbulence, followed by a free-space turbulence simulation representation.

3.1 Numerical Model

The Kolmogorov-Obukhov theory, which relies on the inertial range to describe refractive index fluctuations in free space, thus establishes a modern concept of atmospheric turbulence. Where this inertia range extends from the outer scale $\boldsymbol{L_0}$, which represents the largest eddies in the turbulence, to the

inner scale $\boldsymbol{l_0}$, which represents the smallest dissipative eddies. The effectiveness of this theory was confirmed when Tatarski was able to rely on it to obtain results related to the spread of electromagnetic waves through a turbulent atmosphere. Therefore, we can start the mathematical representation from the basics, which is by expressing the refractive index $\boldsymbol{n(r)}$ of the atmosphere as [18]:

$$n(r) = E[n(r)] + n_1(r), \quad \ldots(1)$$

Where $E[n(r)]$ denotes the ensemble average of the refractive index, which is approximately equal to 1 for the atmosphere, and $n_1(r)$ represents the fluctuating component with $E[n_1(r)] = 0$.

The characteristics of these fluctuations can be described by the structure-function $D_n(r)$, which obeys the Kolmogorov-Obukhov 2/3 law [18]:

$$D_n(r) = E[|n_1(r + r_1) - n_1(r_1)|^2] = C_n^2 r^{-2/3}, \ldots(2)$$

Where the structure, constant C_n represents the strength of turbulence.

The structure-function $D_n(r)$ is related to the covariance function $B_n(r)$ of the refractive index fluctuations as [19]:

$$D_n(r) = 2\big(B_n(0) - B_n(r)\big). \quad \ldots(3)$$

Here, $B_n(0) = E[|n_1(r)|^2]$ is a constant value representing the variance of $n_1(r)$ at a single point, and $B_n(r)$ is the covariance between two points separated by r. As r increases $B_n(r)$ decreases, which means $D_n(r)$ increases with r, characterizing the growing difference in fluctuations as the separation distance grows.

By substituting equation (2) into equation (3) and solving for $B_n(r)$, we get:

$$B_n(r) = B_n(0) - \frac{1}{2} C_n^2 r^{-\frac{2}{3}}. \quad \ldots(4)$$

To understand the energy distribution across different spatial scales in the turbulent atmosphere, it is essential to examine the power spectral density $\Phi_n(k)$, which represents the Fourie rtransform of the covariance function $B_n(r)$, as shown in [19]:

$$B_n(r) = \frac{1}{(2\pi)^3} \iiint_{-\infty}^{\infty} \Phi_n k e^{-ik.r}\, d^3k. \quad \ldots(5)$$

Where $k = |k|$ is the spatial wavenumber r. Taking the Fourier transform of $B_n(r)$ gives us $\Phi_n(k)$ in terms of C_n^2 and the separation distance r.

Within the inertial range, the power spectral density $\Phi_n(k)$ that corresponds to the structure-function $D_n(r) = C_n^2 r^{-2/3}$ will be as in [20]:

$$\Phi_n^K(k) = 0.033 C_n^2 k^{-11/3}. \quad \ldots(6)$$

This expression, known as the Kolmogorov spectrum, describes the energy distribution across spatial frequencies for scales k in the inertial range, where $1/L_0 << k << \frac{1}{l_0}$.

The Kolmogorov spectrum assumes that turbulence eddies exist across an infinite range of scales, which is not physically realistic. In practice, turbulence has finite outer and inner scales, represented by L_0 and l_0, respectively. To account for these limits, we use the von Kármán spectrum, a modified version of the Kolmogorov spectrum that includes scale cutoffs in general as [2•]:

$$\Phi_n^{vK}(k) = 0.033 C_n^2 k^{-11/3} \frac{\exp(-k^2/k_m^2)}{(k^2 + k_0^2)^{11/6}} \quad for\ 0 \leq k < \infty, \quad \ldots(7)$$

With $k_m = 5.92/l_0$ and $k_0 = 2\pi/L_0$, the von Kármán spectrum modifies the Kolmogorov spectrum by including an exponential cutoff $\exp(-k^2/k_m^2)$ to account for the inner scale, and a low-wavenumber suppression term $(k^2 + k_0^2)^{-11/6}$ to represent the outer scale. This formulation captures both the large-scale and small-scale turbulence limits. Starting with the structure function for refractive index fluctuations, we derived the Kolmogorov power spectrum for the inertial range. We then extended this to the von Kármán spectrum, which incorporates the effects of finite inner and outer scales. This comprehensive simulation model is essential to accurately predict the effect of atmospheric turbulence on the optical beam across all relevant scales.

Specific parameters are essential to evaluate the effectiveness and flexibility of optical beams propagating under atmospheric turbulence described by the von Kármán spectrum. This study focuses on three key metrics (scintillation index, Strehl ratio, and overlap) that effectively capture the changes in optical beam shape and intensity under turbulent conditions. These parameters provide valuable insights into the optical beam's stability and coherence, offering a robust assessment of the model's performance in FSO communication.

An optical beam propagating through the atmosphere will experience irradiance (intensity) fluctuations, or scintillation, even over relatively short propagation paths. Scintillation is caused almost exclusively by small temperature variations in the atmosphere, resulting in an index of refraction fluctuations (i.e., optical turbulence). Theoretical and experimental studies of irradiance fluctuations generally center around the scintillation index (normalized variance of irradiance fluctuations) defined by [21]:

$$\sigma_I^2 = \frac{\langle I^2\rangle - \langle I\rangle^2}{\langle I\rangle^2} = \frac{\langle I^2\rangle}{\langle I\rangle^2} - 1, \ldots(8)$$

The quantity I denotes the irradiance of the optical beam and the angle brackets < > denote an ensemble average or, equivalently, a long-time average.

For certain applications in FSO communications, the primary concern may not be imaging quality but rather the maximization of the deposited energy. In such cases, the Strehl ratio (S) serves as a valuable figure of merit. The Strehl ratio is defined as the normalized peak intensity of the point spread function (PSF) and is expressed as follows [22]:

$$S = \frac{I_{real}}{I_{ideal}}, \ldots(9)$$

I_{real} and I_{ideal} represent the intensities at the center of the real point image and the ideal PSF (free from aberrations), respectively. The Strehl ratio provides a measure of the beam's ability to maintain peak intensity in the presence of atmospheric turbulence. A value closer to 1 indicates minimal distortion, meaning turbulence less affects the beam.

It is important to note that while the Strehl ratio traditionally originates from optical design quantifying the ratio between the peak focal spot intensity of an

actual optical system and that of a diffraction-limited system it is adapted in studies of atmospheric turbulence. In this context, the S often uses mean intensity values rather than total intensity. Generally, it serves as a measure of how effectively the optical beam remains well-directed and focused despite the degrading effects of turbulence.

In FSO communication systems, the overlap quantifies the proportion of the initial beam's power that remains within its original spatial mode after propagating through atmospheric turbulence. This metric evaluates the ability of an optical beam to maintain its mode structure affecting the transmitted data.

The mathematical equation for overlap is [23]:

$$\eta = \frac{\left|\iint_{-\infty}^{\infty} E(x,y,z')E'^{*}(x,y,z')dxdy\right|^2}{\iint_{-\infty}^{\infty}|E(x,y,z')|^2dxdy.\iint_{-\infty}^{\infty}|E'(x,y,z')|^2dxdy}, \quad \ldots(10)$$

Where $E(x,y,z')$ refers to the transverse electrical field of the mode propagated a distance z' without turbulence and $E'(x,y,z')$ the mode after propagation through turbulent media, $E^{*}(x,y,z')$ and $E'^{*}(x,y,z')$ are the respective complex conjugates of the fields. The best overlap value for this formula is 1, which means that optical beam maintains its mode, and with increasing turbulences, this value decreases and can reach 0. The random phase fluctuations that optical beam are exposed to in free space cause a change in the intensity distribution of this beam, which leads to a loss in intensity and a change in its distribution and thus leakage to other modes in the initial beam. In FSO communication systems, studying the overlap parameter is important because it provides insight into the robustness of the mode and the state of the original coil of the optical beam despite the disturbance [23, 24].

3.2 Simulation Model

Modeling of atmospheric conditions through computer simulations or in the laboratory has facilitated the investigation and development of optical systems. It also helped us learn more about how optical beams interact with turbulence in the atmosphere. This let us guess what the effects of turbulence would be so we could avoid or lessen their severity.

Over time, many methods have been discovered to simulate atmospheric turbulence in the laboratory, such as turbulence chambers that use heaters and fans to provide turbulent environments or turbulence panels, which are glass panels etched with random phase screens based on the turbulence power spectra. As for modern methods, they depend on SLMs and digital micromirror devices (DMDs) and other similar technologies, that provide greater flexibility by allowing real-time adjustments to turbulence models and parameters. These modern technologies can also support computational simulations, making them a versatile tool [17].

Modeling the von Kármán spectrum with the phase screen technique is functional for simulating atmospheric turbulence in FSO communications. But to increase effectiveness, the von Kármán model and phase screen are used with the split-step method to model the turbulence along the propagation path of the optical beam in free space. Where the disturbance in this method is a set of randomly generated von Kármán phase screens, each one reflecting its own different refractive index fluctuations.

For that this method provides an efficient representation of complex impairments due to disturbances such as (wavefront distortion, intensity scintillation). The use of computational tools and taking into account different height profiles and dynamic refractive index changes in implementing this method provides the possibility of studying and analyzing the accumulated effects of disturbances along the propagation path of optical beams [25].

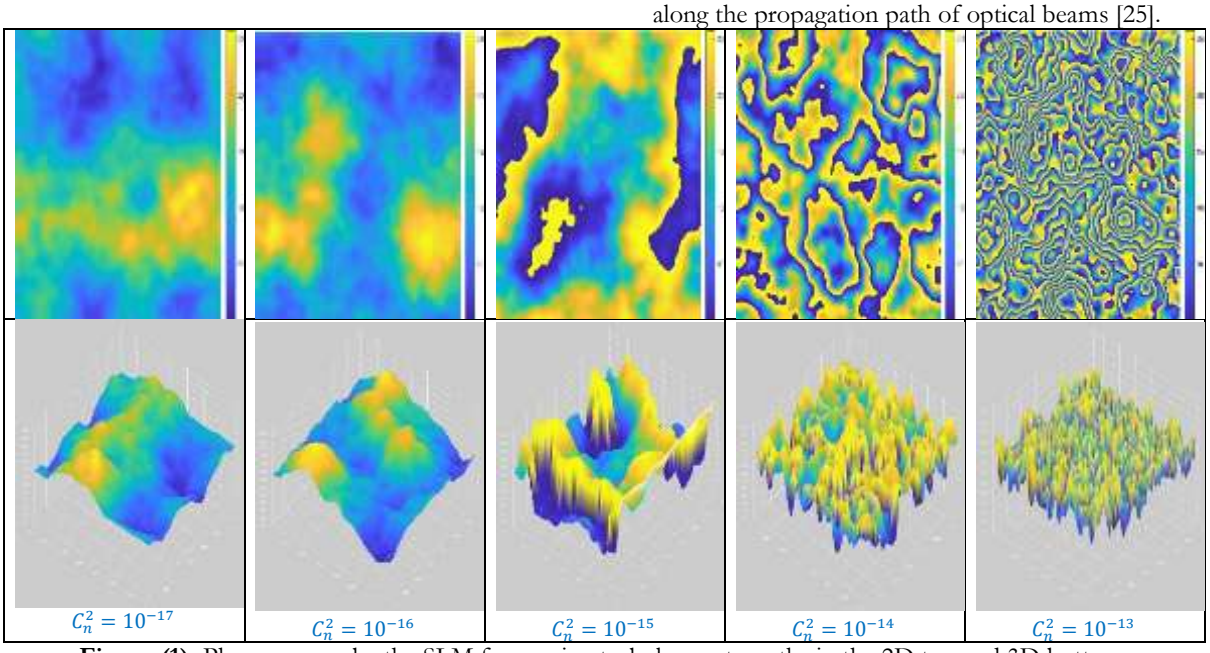

Figure (1): Phase screens by the SLM for varying turbulence strengths in the 2D top and 3D bottom.

To improve this method, raise its efficiency, and make it effective for the communication system proposed in our research, which relies on non-diffracting beams produced once by a traditional

method for the FSO communications system and a second time by the same system, but it uses the optifusion method for protection. Because the results of the two systems may be similar, we need to improve turbulence modeling and precise control.

In this study, we followed a systematic approach to design and simulate a very realistic structure for atmospheric turbulence. consisting of a von Kármán spectrum model, which is the heart of these turbulences and the basis for generating phase screens because it governs their spatial frequency characteristics, while using algorithms to transform the von Kármán spectrum into a physical representation of the turbulence, which is the phase screen, which relies on Fast Fourier Transform (FFT) to simulate random phase screens that reflect atmospheric refractive index fluctuations.

These random phase screens are applied to the path of propagation of the optical beam using the split-step method. Then, the SLM technology displays these phase screens according to the measurements and distances of the split-step method dynamically in the proposed FSO communications system. This structuring of atmospheric turbulence closes the gap between research numerical simulations and physical experiments, thus generating realistic atmospheric turbulence.

The presence of SLM technology in this disturbance structure provides the generation of precise dynamic phase distortions with great flexibility in controlling these generated disturbances. The SLM in the proposed FSO communication system works as a dynamic interface that generates phase screens that impose random phase fluctuations on the optical beam falling on it. These phase distortions will simulate the flickering, scattering, and wavefront curvature that optical beams experience when shining on the SLM. Thus, the SLM in this structure is the part related to command and control, but the basis of the disturbance is the von Kármán model, which is mathematically represented by the modified power spectrum $\Phi_n^{vK}(k)$. Realistic atmospheric conditions as (temperature, wind, pressure) can be represented by the refractive index structure constant C_n^2. The precise control and calculation of these parameters allow the generation of a different range of weather conditions, ranging from mild disturbances to severe distortions.

A non-diffracting beams propagation path is generated in this FSO communications system that is precisely similar to the real world by relying on the split-step method, which determines the number of phase screens and their locations on the path according to the distance over which the optical beams will be propagated and the weather conditions chosen for this distance to reflect the nature, spectral, and cumulative real atmospheric turbulence. Thus, the phase screens refer to the wavefront distortions that scatter the optical beam, interfere with it, and change the intensity distribution and spatial coherence according to the propagation distance and the strength of the disturbance. Thus when an optical beam propagates through this simulation of a turbulent environment, it undergoes changes in its coherence, intensity, and shape depending on the propagation distance and strength of the turbulence. This proposed structure for simulating atmospheric turbulence combines the detailed representation of wavefront dynamics and the flexibility of digital modulation.

In Fig.1, examples of simple and complex random phase screens appear, which were created using the previous approach, based on the von Karman spectrum model, and using the SLM technique, and at different disturbance intensities, starting from weak turbulence strength $C_n^2 = 10^{-17}$ and gradually increasing to strong turbulence at $C_n^2 = 10^{-13}$ passing through moderate turbulence at $C_n^2 = 10^{-15}$. Due to the flexibility of SLM technology, control is easily achieved to simulate different weather environments. Thus, by providing the SLM with realistic parameter values, it generates various scenarios from the sky clear to snow and rain. This simulation provides an efficient and accurate platform to study the effects of free space and atmospheric turbulence on non-diffracting beams at long-range propagation distances in the proposed FSO communication system.

4. Non-Diffracting Beams after Optifusion Method

Why non-diffracting beams because they maintain their transversal intensity profile without spreading as they propagate, remaining "diffraction-free" over significant distances. This characteristic is achieved by structuring the beam such that its component plane waves acquire identical phase shifts, allowing the beam to preserve its form consistently along its propagation path [26].

The general framework for non-diffracting beams begins with the concept of diffraction-resistant or localized waves that maintain their shape during propagation. These beams are solutions to the Helmholtz equation, with their specific forms determined by the coordinate system employed. The Following outlines the unified approach to deriving the general equation for non-diffracting beams across various coordinate systems [27]:

$$\nabla^2\Psi + k^2\Psi = 0\,, \quad \ldots(11)$$

Ψ is the beam's complex, and k is the transverse wave number. For non-diffracting beams, separable solutions are sought in different coordinate systems.

The main types of non-diffracting beams arise from cylindrical and elliptical cylindrical coordinate systems. A general way to represent non-diffracting beams is by integrating them over an angular spectrum. The integral form is [28],

$$\Psi(\mathrm{r},\phi,\mathrm{z}) = \frac{ik}{2\pi}\int_{-\pi}^{\pi} A(\psi)e^{i\alpha r\cos(\psi-\phi)}e^{-i\beta z}\,d\psi, \quad (12)$$

This general formula combines solutions to the Helmholtz equation in an angular spectrum formulation, where the function $A(\psi)$ defines the specific type of non-diffracting beams by controlling the amplitude and phase distribution across the angular spectrum. The parameters α and β of the non-diffracting beam represent projections of the components of plane-wave vectors of the angular spectrum in the transverse plane (x, y) and to the normal of the transverse plane, i.e., the z-axis,

respectively, i.e., $\alpha = ksin\theta_0$ and $\beta = kcos\theta_0$ with $k = 2\pi/\lambda$ the wavevector.

Compared to standard optical beams, non-diffracting beams essentially add a number of features to the FSO communication system, the most important of which is that, first, their distinctive shapes provide an added layer of security for the communication system. Second, they exhibit resistance to atmospheric turbulence, allowing them to maintain their distinctive shapes over long distances. In addition, these non-diffracting beams have a set of characteristics common to all species and others unique to certain species.

General properties, such as diffraction-free propagation, which maintains a constant tangential intensity at distances beyond the Rayleigh range of conventional Gaussian beams, are achieved by the unique structure of each beam. Another feature of many non-diffracting beams is their self-healing capability.

When these beams encounter an obstruction, they can reconstruct their original transverse profile upon further propagation. Some non-diffracting beams have unique properties, such as the Airy beam, which exhibits self-acceleration along a curved path, in contrast to the straight-line propagation of optical beams. Furthermore, non-diffracting beams can carry phase singularities as in vortex beams, granting them angular momentum, and they may also display self-imaging properties, allowing them to recreate their profile periodically during propagation [9, 29]. These distinctive attributes make non-diffracting beams invaluable across various fields, particularly optical communication.

We can classify the methods for generating non-diffracting beams into three main methodologies. The first are standard optical components, such as axicons. The second, and most widely used, is SLMs, which offer a versatile and effective solution for generating various non-diffracting beam types. The third methodology employs nonlinear techniques [9, 29].

In this study, we utilize three types of non-diffracting (Bessel–Gauss, Finite-energy Airy, and non-diffracting vortex) beams selected for their diverse characteristics, effectiveness, and varying levels of efficiency in free-space propagation. These beams are generated using SLM technology and a Gaussian beam source. Directing a Gaussian beam onto the SLM and employing the corresponding hologram can produce any desired non-diffracting beam. Modulating the Gaussian beam into these non-diffracting beam forms allows us to create energy-limited versions of the three beam types, based on the Gaussian beam's finite energy rather than the idealized infinite-energy models. This approach ensures a practical simulation of real-world scenarios.

This proposed approach allows an in-depth analysis of the influence of the optifusion method and atmospheric turbulences on non-diffracting beams that mask data when it is propagation in free space.

The results gained from this simulation experiment will contribute to developing the optifusion method and improve our understanding of the interactions of non-diffracting beams with atmospheric turbulence.

In Fig.2, we observe the three non-diffracting (Bessel–Gauss, Finite-energy Airy, and non-diffracting vortex) beams generated from the Gaussian beam by SLM in terms of their wavefront and cross-section immediately after being in the free space after carrying and hiding the data using the optifusion method. These initial shapes serve as a reference for subsequent comparisons after they simulate their propagation through free space, where they are exposed to atmospheric turbulence specifically designed by the free-space turbulence simulation model created in the previous section. By analyzing these non-diffracting beams before and after exposure to turbulence and carrying data with and without the optifusion method.

Based on the simulation results of the proposed system, several analyses can be drawn. These conclusions can include the quality of the optifusion method with non-diffracting beams, determining which non-diffracting beams perform best, the conditions under which they are most effective, and the distances at which they remain optimal. In addition, the quality of the free-space channel, the disturbances simulated, and whether these disturbances created real effects can be inferred and evaluated. Where this system relies on an optifusion method to enhance security and non-diffracting beams to increase propagation distance and resistance to atmospheric turbulence.

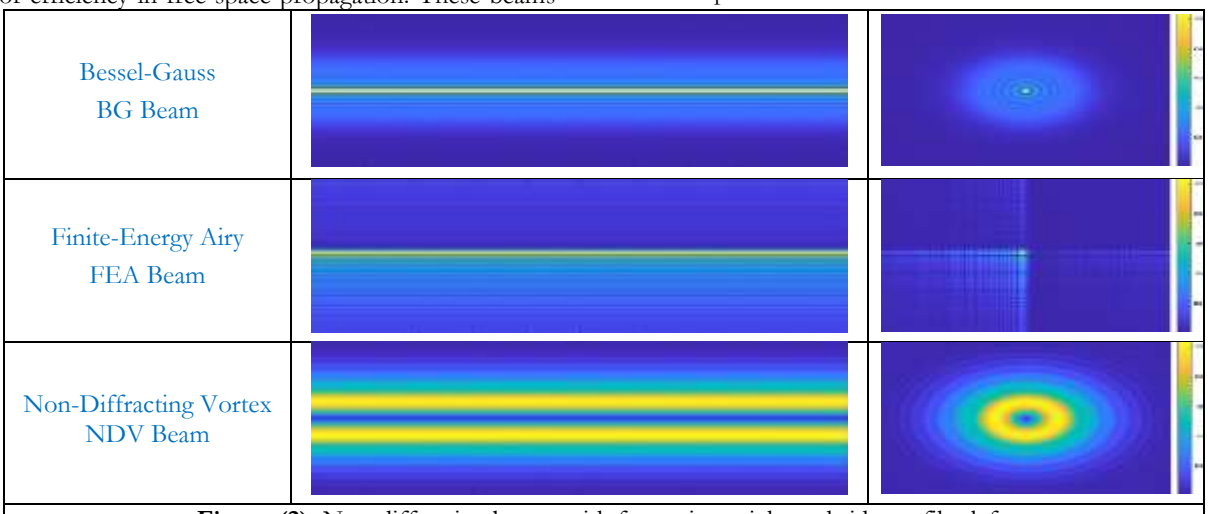

Figure (2): Non-diffracting beams with front views right and side profiles left.

5. System Simulation

The comprehensive simulation of the proposed optical communication system is illustrated in Fig.3. These beams can be generated and controlled dynamically by adjusting the hologram in the SLM. These beams propagate through a free-space medium under the influence of various atmospheric turbulence, which are simulated and controlled by using another SLM.

The most effective component of this system is the SLM technology through which we generated the non-diffracting beams and the atmospheric turbulence. Where SLM is a dynamic optical technique that modulates the properties of light, such as phase and amplitude, on a spatial grid, allowing precise control of the light wavefront. SLMs can be classified into amplitude-modulating and phase-modulating types.

Phase-modulating SLMs, especially phase-only SLMs are based on reflective and are highly effective in beam shaping and adaptive optics. Phase-only reflective SLMs employ liquid crystal-on-silicon (LCoS) technology, allowing them to achieve high spatial resolution and efficient phase modulation, making them ideal for structured light applications [30]. Therefore, in this study, phase-only reflective SLMs were used because they, in addition, offer major advantages of FSO systems, such as high precision in phase control, minimal light loss, and compatibility across different wavelengths. Their ability to maintain high efficiency in modulating the phase enables applications requiring robust control over beam shape, which is crucial in this optical communication system [30].

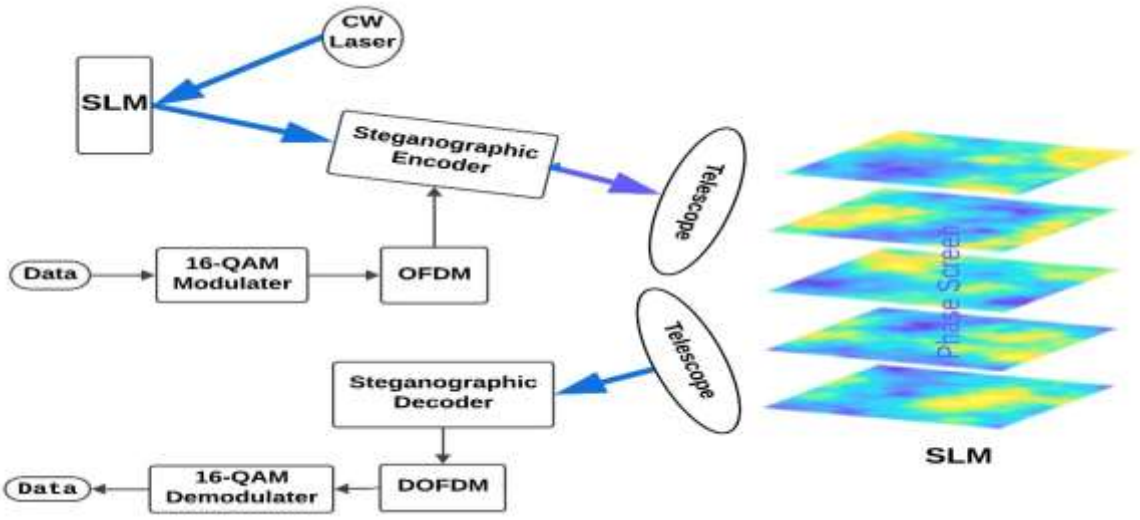

Figure (3): Flowchart to simulate an optical communication system in free space under different turbulence.

The proposed system utilizes a diode laser operating at a wavelength of 1550 nm, emitting a Gaussian beam directed toward a phase-only reflective SLM. By encoding holograms of the three selected types of non-diffracting beams into the SLM, the desired beams can be generated. Precise control of the SLM parameters allows tuning of the characteristics of these beams. In this study, pseudo-random data is hidden in the non-diffracting beams by using an optifusion steganographic encoder. The data is modulated via quadrature amplitude modulation (QAM) and orthogonal frequency-division multiplexing (OFDM) technology into an OFDM signal, which is then masked within the non-diffracting beam. These non-diffracting beams are transmitted through free space using a high-resolution transmission telescope.

By using the second phase-only reflective SLM to create the free space and its turbulence. Which introduces disturbances similar to those that occur in the real world by adjusting its parameters. In order to obtain accurate results for the propagation of non-diffracting beams in free space and under the influence of disturbances to the proposed communication system, it is necessary to adjust the propagation distance z with the number of phase screens and the spacing between them, the refractive index structure C_n^2, and the power spectral density Φ_n.

And by using a modified algorithm, it depends on the parameters the (z, C_n^2 and Φ_n) as inputs to generate the random phase screens and their numbers, spacing, and dimensions that correspond the dimensions of the non-diffracting beams used in this simulation. This is help to reduce side effects, losses, and inaccurate results that occur due to the incompatibility of the size of the optical beams with the random phase screens and the carrier medium, and thus enhance the accuracy of the results obtained. Also, the SLM is also programmed to create a controlled environment that realistically replicates atmospheric deformations.

In the reception system, the telescope with high sensitivity receives the non-diffracting beams after propagation in free space and its exposure to various turbulence. These non-diffracting beams experience distortions in shape and intensity due to the distance traveled and the strength of atmospheric disturbances. Such distortions directly affect the process of extracting the hidden data.

The optifusion steganographic decoder retrieves the OFDM signal, which is demodulated by QAM and DOFDM to reconstruct the transmitted data. A key

advantage of this system is its ability to encode and decode data directly within the non-diffracting beams, eliminating the need for conversion to or from Gaussian beams. Furthermore, prior knowledge of the encoding process along with the location, size, and specific parameters of the hidden data ensures efficient and accurate data extraction.

When modeling the propagation of the three non-diffracting (BG, FEA, and NDV) beams under varying levels of atmospheric turbulence, their effectiveness and quality are observed in terms of maintaining their shape and intensity after propagation through free space. These beams exhibit strong resilience to weak disturbances, preserving their structure over distances exceeding 10 km. However, under severe turbulence, significant deformation occurs even at short propagation distances lower than 1km, as illustrated in Fig.4. The interaction of these beams with free-space conditions varies depending on the intensity of the turbulence. These preliminary results are consistent with those reported in the literature, confirming the accuracy of the secure optical communications system using the optifusion method with non-diffracting beams, free-space environments, and atmospheric turbulence.

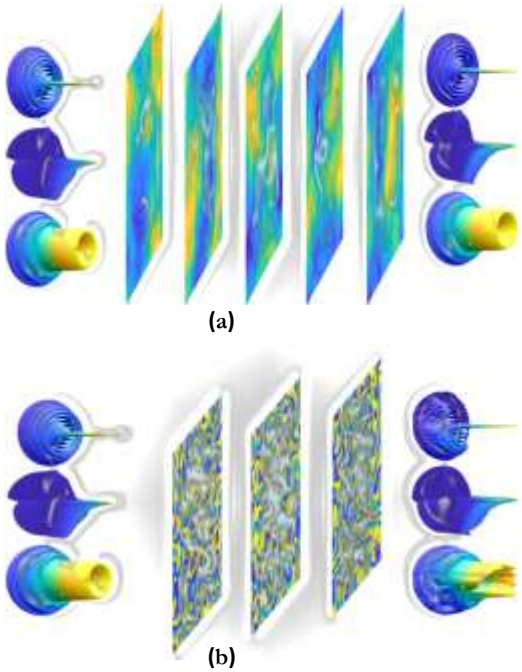

Figure (4): Modeling the propagation of non-diffracting (BG, FEA, and NDV) beams in free space under the influence of (a) Weak and (b) strong turbulence.

6. Result Analysis:

In this study, several objectives were implemented, and to verify them, the results obtained will be analyzed. The primary goal was to evaluate the quality and performance of the optifusion method when applied to non-diffracting beams in the FSO communication system. This was achieved by comparing the results of the proposed system, which employs the optifusion method, with those of a standard system where data is not hidden under identical conditions same non-diffracting beam types, propagation distances, and weather conditions. Another objective was to check the most suitable beam type among the three non-diffracting beams considered in this study, based on their compatibility with the optifusion method in the same conditions. This will be verified by analyzing the performance of these non-diffracting beams under identical environmental and deployment scenarios. Additionally, this study aimed to evaluate the transmission medium and the effects of atmospheric turbulence, which were meticulously modeled in the simulation to replicate real-world conditions. Studying and analyzing the results of the impact of disturbances on the non-diffracting beams of the FSO communication system helps in avoiding and overcoming these turbulences in the real world.

The values (scintillation index, Strehl ratio, and overlap) of non-diffracting beams help in evaluating the efficiency of these beams when propagating in free space from one side, and from another side, these values examine the quality of turbulence simulation in the effect on these turbulence-resistant beams. These parameters also help in comparing between the three types of selected non-diffracting beams in terms of shape and intensity in two scenarios of the same FSO communication system with and without the optifusion method. In this study, we rely on the values of these three parameters because they evaluate the stability of the non-diffracting beam, the quality of its intensity, and its spatial coherence when exposed to disturbances.

The scintillation index parameter focuses on the scintillation, brightness changes, and fluctuations in the intensity of non-diffracting beams after exposure to atmospheric turbulence and along the propagation path in free space. Since its best value is zero or close to zero, and it occurs when there are no disturbances, i.e., in an ideal environment, or when the non-diffracting beam begins to leave the sender system and enter into free space, and this value increases with the increase in turbulence or its accumulations when the propagation distance increases. Based on equation (8), we sampled the scintillation index parameter to non-diffracting beams at different propagation distances and weather conditions. One of the principles examining optical beams after they are exposed to disturbances when they propagate is to compare the intensity of this beam under ideal conditions, that is, when it is not exposed to turbulence with the same beam, but after it is exposed to turbulence at the same distance; this comparison is made by calculating the Strehl ratio parameter. The best value for the Strehl ratio is 1 under ideal conditions and decreases as the effect of disturbances on the optical beam increases. The Strhel ratio values for the selected non-diffracting beams were calculated by equation (9). Because non-diffracting beams have distinct shapes, these shapes can be lost due to overlapping modes when subjected to disturbances, which subsequently affects their stability and energy when they continue to spread in free space. Therefore, the overlap parameter was chosen, which compares the modes of the non-diffracting beam when entering and leaving from free space. The value of the overlap parameter at the

beginning of the transmission is 1 and decreases with increasing propagation distance and turbulence, as its values were calculated in this research using the equation (10).

To cover most of the weather conditions that the proposed FSO communications system would be exposed to in the real world. We will simulate natural, extreme environments and what's in between. The natural environment has weak turbulences, such as light fog or light wind, which can be represented at a turbulence strength $C_n^2 = 10^{-17}$. As for the environment with moderate turbulence, such as dense fog or strong winds, it is represented at the strength of the turbulence $C_n^2 = 10^{-15}$. Harsh environments such as snow and rain can be shown at turbulence strength $C_n^2 = 10^{-13}$, which represents strong turbulence.

The results of the influence of these environments on the non-diffracting beams (BG, FEA, and NDV) of the proposed FSO communication system with and without the optifusion method were studied and analyzed. Performance evaluations were conducted at a propagation distance of 10 km, representing long-range communication. This distance allows evaluating the quality of representation and simulation of the medium when the effect of atmospheric turbulence accumulates with increasing propagation distance.

In Fig. 5, the results of the scintillation index for non-diffracting (BG, FEA, and NDV) beams with and without the optifusion method in these environments. The weak turbulence scenario in Fig. 5(a) shows the scintillation index values for the non-diffracting beams in the conventional manner, identical to the scintillation values for the same beam but in the optifusion manner. These results prove that the optifusion method does not affect the shape and intensity and characteristics of the non-diffracting beams. The performance of the BG beam is also slightly better than the other beams, as it offers minimal brightness variation. As for the simulation of the conducting medium, it provides stability in persistent weak turbulence along propagation distances. This indicates that the deflected beams maintain their intensity at minimal fluctuations.

In the moderate turbulence scenario depicted in Fig. 5 (b), the scintillation index values for the non-diffracting beams with the optifusion method remain closely aligned with those of the same beams without it, even as atmospheric turbulence intensifies. Among non-diffracting beams, the NDV beam outperforms the BG beam very slightly due to the stability of this type of beam due to its reliance on OAM, which enables it to compete with BG beams in resisting disturbances, while the FEA beam appears less efficient in terms of scintillation due to its non-uniform intensity distribution. In contrast, the regular structures of the BG and NDV beams are better suited for controlling scintillation. The quality of modeling of the free-space medium is demonstrated by continuously calculated turbulences along the propagation path that lead to a gradual increase in the scintillation index values of all non-diffracting beams.

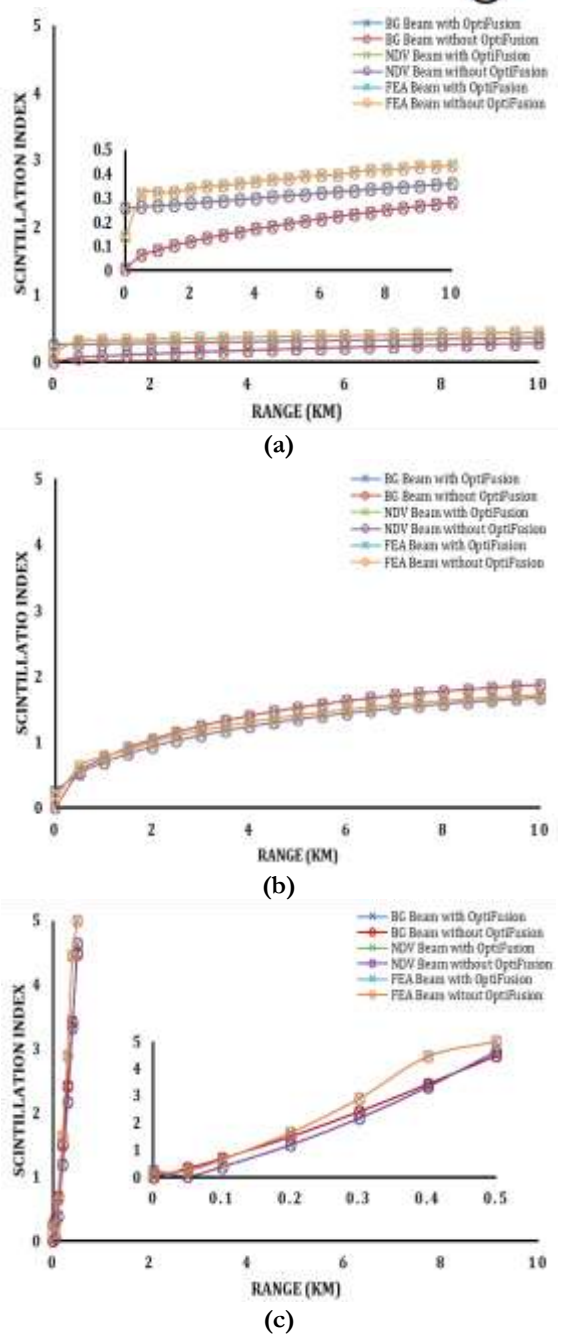

Figure (5): Scintillation index for non-diffracting (BG, FEA, and NDV) beams with and without the optifusion method under (a) weak, (b) moderate, and (c) strong turbulence.

In the third scenario Figure 5(c), with very high atmospheric turbulence, the optifusion method still proves its robustness, as the scintillation index values for non-diffracting beams with and without optifusion remain closely matched. Notably, the BG and NDV beams perform comparably well in these conditions, showing strong resistance to turbulences and brightness loss. However, due to the intense disturbances, the medium's effects become pronounced, causing significant intensity loss and beam dispersion. Notably, after approximately 500 m, strong turbulence leads to substantial non-diffracting beam distortion and degradation.

Fig.6 presents the Strehl ratio values for the selected scenarios, comparing the shapes of the non-

diffracting beams under identical weather conditions and propagation distances to their ideal shapes. The results show that, in all scenarios, the Strel ratios remain similar or very close for non-diffracting beams once using the optifusion method and for the same beams without this method. This consistency highlights the strength of the optifusion method in preserving the shapes and properties of the optical beam when hiding data within it, in addition to confirming what was stated in the literature about the strength of non-diffracting beams in maintaining their shapes over the propagation distance despite atmospheric turbulences.

Under weak and moderate turbulence conditions, as shown in Fig.6 (a and b), the Strehl ratio values for all non-diffracting beams remain near 1, indicating excellent beam stability and shape preservation. This demonstrates the efficiency of non-diffracting beams in maintaining their original shape despite turbulence. Among the non-diffracting beams, the BG beam achieves the highest Strehl ratio, followed by the NDV beam, while the FEA beam shows slightly lower values but remains comparable. These results emphasize the superior performance of the BG beam as atmospheric disturbances intensify.

Fig. 6(c) illustrates the Strehl ratio results under strong turbulence. The intensities of non-diffraction beams are subjected to significant distortion in this scenario at a distance of less than 500 m, and thus it is difficult to compare it to itself in the ideal case for calculating Strehl ratio values at a distance greater than 500 m. Within a propagation distance of less than 500 m, the Strehl ratio values for all beams remain close due to distortion due to instantaneous and intense turbulence, with little cumulative distortion due to the short propagation distance. The FEA beam produces the lowest Strehl ratio values, as it is the fastest and most distorting of the beams and thus the least effective, followed by the NDV beam, while the BG beam shows a slight advantage by propagating for approximately 500 m before becoming distorted, indicating better flexibility in the face of turbulences. The Strehl ratio in these scenarios demonstrated the efficiency of simulating free space and its turbulence through its precise effect on the initial intensity of the non-diffracting beams. When comparing the intensity of non-diffracting beams before and after they were exposed to the same disturbances, we find that the values of the Strehl ratio were logical and close to reality. Furthermore, the medium effectively replicated severe weather scenarios, accurately detecting the distortion of non-diffracting beams beyond 500 m. Additionally, the simulated environment provided a reliable framework for assessing each beam's resilience in preserving its shape during propagation.

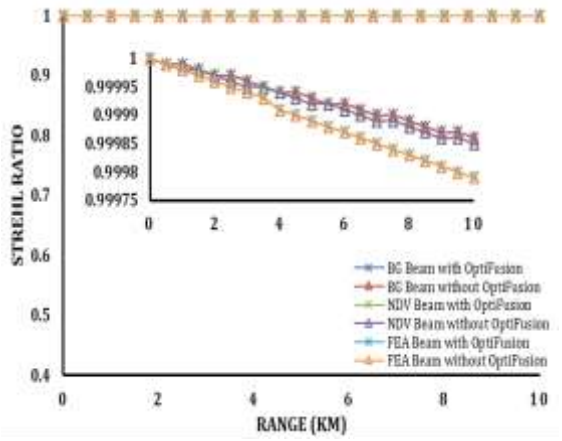

(a)

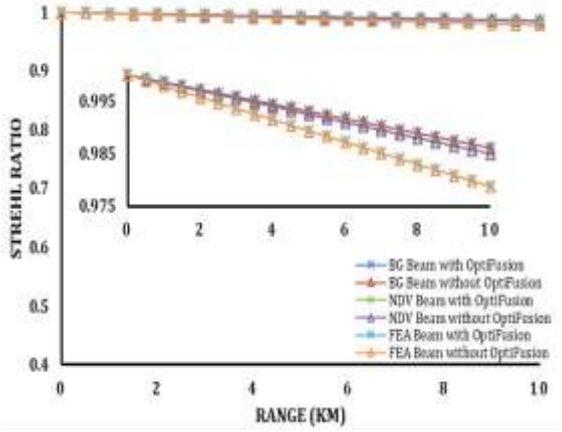

(b)

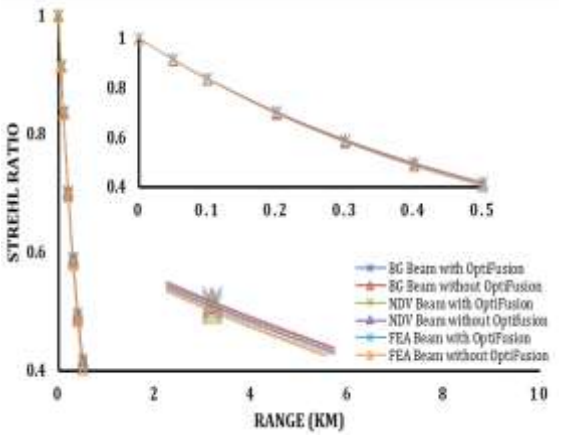

(c)

Figure (6): Strehl ratio for non-diffracting beams (BG, FEA, and NDV) with and without the optifusion method under (a) weak, (b) moderate, and (c) strong turbulence

Calculating the overlap parameter values for the non-diffracting beams with or without the optifusion method in the three scenarios shows the structural integrity of the non-diffracting beams modes when they enter and leave the transmission medium and after they are exposed to atmospheric disturbances. It also provides insight into the efficiency of these beams to retain their energy after encountering atmospheric turbulence.

Using non-diffracting finite energy beams, this study creates an accurate model to evaluate energy dissipation during propagation in a free-space

simulation. The results obtained for the overlap, in Fig.7, confirmed the effectiveness of the proposed simulation system and that the transmission medium had a consistent and logical effect on the non-diffracting beams, yielding results that align with real-world conditions. While atmospheric turbulence had a uniform impact under similar conditions, variations in reception were observed due to differences in beam shapes, modes, and energy distributions.

The study revealed that overlap primarily arises from beam distortions, which alter the fundamental structure of non-diffracting beams. This includes lateral mode overlap and irregular interactions between modes, caused by non-uniform turbulence. The overlap values further highlighted the rates of energy loss during propagation, showing that energy dissipation varies between non-diffracting beam types under identical conditions. These findings provide additional evidence of the logical and consistent nature of the results.

The optifusion method has confirmed its efficiency again and now with the overlap parameter, as shown in Fig.7, where the overlap values for these non-diffracting beams, with and without the optifusion method across three turbulence scenarios are similar or very close. Under weak turbulence conditions, Fig.7 (a) shows that the FEA beam showed a significantly faster rate of energy loss and mode distortion than the BG and NDV beams. However, the overlap values of the BG and NDV beams remained close to 1, highlighting their robustness under such conditions.

Analysis of these results shows that beams with irregular shapes experience greater energy loss, rapid distortion, and overlap of their modes, like the FEA beam. In contrast, beams with regular or symmetrical structures, such as BG and NDV, showed slower energy dissipation and minimal mode overlap. In moderate turbulences, Fig.7 (b) the energy loss and mode distortion were similar to the weak turbulences scenario for all non-diffracting beams, with a slight superiority for the BG beam over the NDV beam. Where the BG and NDV beams continued to perform competitively due to their distinct structural advantages.

While the BG beam exhibited strong resistance to turbulence, the NDV beam leveraged its central wide ring structure to reduce overlap and maintain performance. In the strong atmospheric turbulence scenario, Fig.7(c), all non-diffracting beams suffered significant energy loss, mode distortion, and very rapid structural deterioration at short propagation distances. Despite the very similar overlap values for all non-diffracting beams in this scenario because they propagate over short distances and deteriorate quickly, the BG beam showed slightly better performance due to its high resistance against strong turbulences.

From the results obtained and analyzed, the simulation system used to model the free-space transmission medium and atmospheric turbulence has proven effective and consistent with the literature, accurately reflecting real-world transmission effects. The results also confirmed the efficiency of the optifusion method, as the three parameters showed almost identical values when transmitting data conventionally or hidden within non-diffracting beams. The results also highlight the robustness of the selected non-diffracting beams in resisting atmospheric turbulences and spreading over long distances while keeping the data hidden within them.

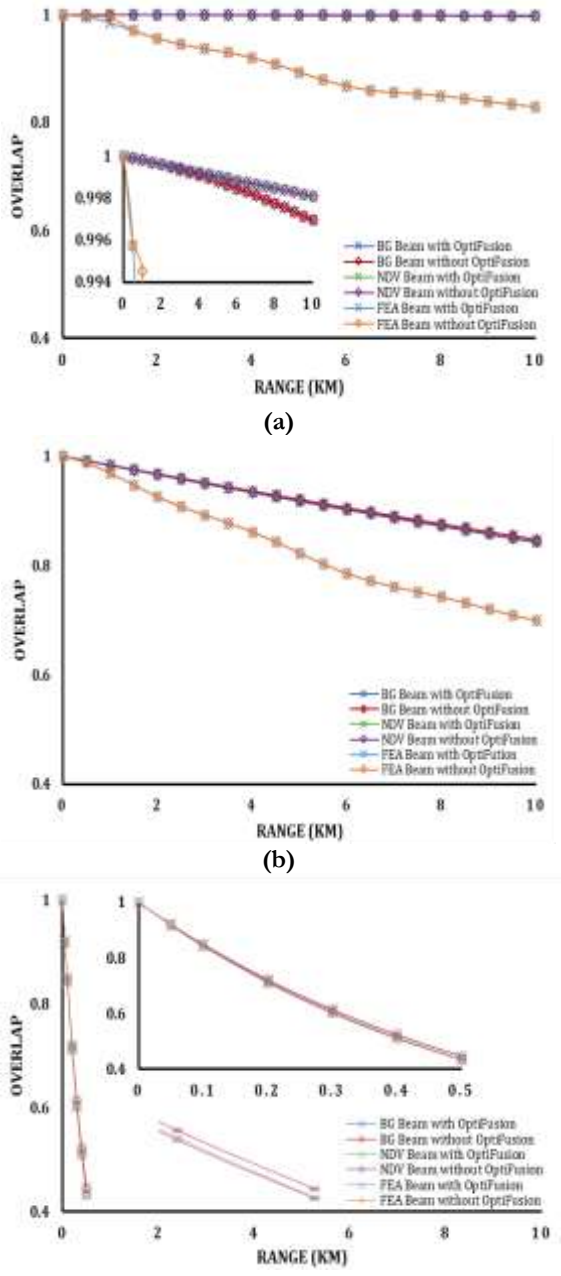

Figure (7): Overlap for non-diffracting beams (BG, FEA, and NDV) with and without the optifusion method under (a) weak, (b) moderate, and (c) strong turbulence.

7. Conclusion

This study simulated an FSO communication system with the optifusion method and effectively non-diffracting beams. The atmospheric turbulence simulation used contributed to the analysis of this system and produced distinctive results that enhanced the evaluation process. The results demonstrate the effectiveness of the optifusion method, indicating that the performance of a communication system using it

is very close to that of an optical communication system without it, indicating that its implementation of protection does not affect the efficiency of data transmission.

The non-diffracting (BG, FEA, and NDV) beams demonstrated excellent data transfer quality and protection under varying disturbance levels, with or without the optifusion method. BG beam has demonstrated remarkable stability and resilience to large disturbances, protecting the data within them. The performance of the NDV beam was similar to the BG beam but slightly inferior, while the FEA beam, since it was more susceptible to distortion due to its irregular shape and uneven intensity distribution, showed the lowest performance among all the beams.

We relied on calculating the values of performance metrics (scintillation index, Strehl ratio, and overlap) to show the accuracy of the proposed optical system. The results confirmed the feasibility of integrating non-diffracting beams with data hiding techniques to improve the security and adaptability of FSO communications systems in different weather conditions.

8. References:

[1] H. M. Razaq and W. K. Saad, "Review of Free Space Optical Communication: Advantages and Disadvantages," in *Proc. 10th Int. Conf. Wireless Netw. Mobile Commun. (WINCOM)*, Istanbul, Turkey, Oct. 2023, pp. 1–5. doi: 10.1109/WINCOM59760.2023.10322932.

[2] A. K. Majumdar, *Advanced Free Space Optics (FSO): A Systems Approach*, 1st ed., Springer Series in Optical Sciences. New York, NY, USA: Springer, 2015. doi: 10.1007/978-1-4939-0918-6.

[3] S. Sawhil, S. Agarwal, Y. Singhal, and P. Bhardwaj, "An Overview of Free Space Optical Communication," *Int. J. Eng. Trends Technol. (IJETT)*, vol. 55, no. 3, pp. 120–125, Jan. 2018. doi: 10.14445/22315381/IJETT-V55P223.

[4] Z. Zalevsky, G. S. Buller, T. Chen, M. Cohen, and R. Barton-Grimley, "Light detection and ranging (LiDAR): introduction," *J. Opt. Soc. Am. A*, vol. 38, no. 11, pp. LID1–LID2, Nov. 2021. doi: 10.1364/JOSAA.445792.

[5] S. Mane, "Overview on Remote Sensing Technologies: Challenges and Applications," ASTROEX Research Association, Dec. 2022. [Online].Available:https://www.researchgate.net/publication/366216574.

[6] M. C. Roggemann and B. M. Welsh, *Imaging Through Turbulence*, 1st ed. Boca Raton, FL, USA: CRC Press, 1996. doi: 10.1201/9780203751282.

[7] D. C. Cowan, J. Recolons, L. C. Andrews, and C. Y. Young, "Propagation of flattened Gaussian beams in the atmosphere: a comparison of theory with a computer simulation model," *Proc. SPIE - Atmospheric Propagation III*, vol. 6215, pp. 62150B, 2006. doi: 10.1117/12.669601.

[8] J. P. Amaral, J. C. A. Rocha, E. J. S. Fonseca, and A. J. Jesus-Silva, "Method to define non-diffracting optical beams mimicking the shape of simple plane curves," *Appl. Opt.*, vol. 58, no. 13, pp. 3659–3663, 2019. doi: 10.1364/AO.58.003659.

[9] Y.-X. Ren, H. He, H. Tang, and K. K. Y. Wong, "Non-diffracting light wave: Fundamentals and biomedical applications," *Front. Phys.*, vol. 9, Art. 698343, 2021. doi: 10.3389/fphy.2021.698343.

[10] K. H. Kadem and M. F. Mohammed, "OptiFusion steganography method based on masking OFDM signal in Gaussian beam intensity," *J. Opt.*, Oct. 2024. doi: 10.1007/s12596-024-02253-7.

[11] S. Sahoo, C. Panda, U. Bhanja, "Performance evaluation of an OFDM-FSO-steganography model, in 2023 International Conference on Microwave," *Optical, and Communication Engineering (ICMOCE), IEEE*, 2023, pp. 1-6. doi: 10.1109/ICMOCE57812.2023.10166349.

[12] H. Song, A. Almaiman, H. Song, Z. Zhao, R. Zhang, K. Pang, C. Liu, L. Li, K. Manukyan, S. Zach, N. Cohen, M. Tur, A.E. Willner, "Hiding a low-intensity 50-Gbit/s QPSK free-space OAM beam using an orthogonal co-axial high-intensity 50-Gbit/s QPSK beam," *Appl. Opt*, 2020. doi: 10.1364/AO.396386.

[13] R. K. Tyson and B. W. Frazier, *Field Guide to Adaptive Optics*, 2nd ed., vol. FG24. Bellingham, WA, USA: SPIE Press, 2012. doi: 10.1117/3.923078.

[14] F. Wang, W. Du, Q. Yuan, D. Liu, and S. Feng, "A survey of structure of atmospheric turbulence in atmosphere and related turbulent effects," *Atmosphere*, vol. 12, no. 12, pp. 1–14, Dec. 2021. doi: 10.3390/atmos12121608.

[15] L. C. Andrews and R. L. Phillips, *Laser Beam Propagation through Random Media*, 2nd ed. Bellingham, WA, USA: SPIE Press, 2005, pp. 11–366. doi: 10.1117/3.626196.

[16] F. L. dos Santos, L. Botero-Bolívar, C. H. Venner, and L. D. de Santana, "Modelling the Dissipation Range of von Kármán Turbulence Spectrum," in *AIAA AVIATION Forum*, Aug. 2021, pp. 1–18. doi: 10.2514/6.2021-2292.

[17] M. A. Cox, N. Mphuthi, I. Nape, N. P. Mashaba, L. Cheng, and A. Forbes, "Structured light in turbulence," *IEEE J. Sel. Topics Quantum Electron.*, vol. 27, no. 2, pp. 7500521, Mar. 2021. doi: 10.1109/JSTQE.2020.3023790.

[18] K. S. Shaik, "Atmospheric Propagation Effects Relevant to Optical Communications," *TDA Prog. Rep.*, vol. 42-94, Jet Propulsion Laboratory, California Institute of Technology, Apr.–Jun. 1988.[Online].Available:https://ntrs.nasa.gov/citations/20040191353.

[19] N. Blaunstein and N. S. Kopeika, *Optical Waves and Laser Beams in the Irregular Atmosphere*. Boca Raton, FL, USA: CRC Press, 2018. ISBN: 978-1-138-10520-1.

[20] L. C. Andrews, "An Analytical Model for the Refractive Index Power Spectrum and Its Application to Optical Scintillations in the Atmosphere," *J. Mod. Opt.*, vol. 39, no. 9, pp. 1849–1853, 1992. doi: 10.1080/09500349214551931.

[21] L. C. Andrews, R. L. Phillips, and C. Y. Young, *Laser Beam Scintillation with Applications*. Bellingham, WA, USA: SPIE Press, 2001, ch. 2. doi: 10.1117/3.412858.ch2.

[22] M. Alavinejad, B. Ghafary, and F. D. Kashani, "Analysis of the propagation of flat-topped beam with various beam orders through turbulent atmosphere," *Opt. Lasers Eng.*, vol. 46, no. 1, pp. 1–5, Jan. 2008. doi: 10.1016/j.optlaseng.2007.07.003.

[23] J. Demas, L. Rishøj, and S. Ramachandran, "Free-space beam shaping for precise control and conversion of modes in optical fiber," *Opt. Express*, vol. 23, no. 22, pp. 28531–28543, Nov. 2015. doi: 10.1364/OE.23.028531.

[24] R. Brüning, Y. Zhang, M. McLaren, M. Duparré, and A. Forbes, "Overlap relation between free space Laguerre Gaussian modes and step-index fiber modes," *J. Opt. Soc. Am. A*, vol. 32, no. 6, pp. 1024–1031, Jun. 2015. doi: 10.1364/JOSAA.32.001678.

[25] Y. K. Chahine, S. A. Tedder, B. E. Vyhnalek, and A. C. Wroblewski, "Beam propagation through atmospheric turbulence using an altitude-dependent structure profile with non-uniformly distributed phase screens," *Proc. SPIE*, vol. 11272, pp. 1127215-1–1127215-12, 2020. doi: 10.1117/12.2543583.

[26] M. Mazilu, D. J. Stevenson, F. Gunn-Moore, and K. Dholakia, "Light beats the spread: 'non-diffracting' beams," *Laser Photon. Rev.*, vol. 4, no. 4, pp. 529–537, Sep. 2010. doi: 10.1002/lpor.200910019

[27] T. A. Vieira, I. S. V. Yepes, R. A. B. Suarez, M. R. R. Gesualdi, and M. Zamboni-Rached, "Optical reconstruction of non-diffracting beams via photorefractive holography," *Appl. Phys. B*, vol. 123, no. 134, pp. 1–12, 2017. doi: 10.1007/s00340-017-6711-1.

[28] Z. Bouchal, "Nondiffracting optical beams: Physical properties, experiments, and applications," *Czechoslovak J. Phys.*, vol. 53, no. 7, pp. 535–542, Jul. 2003. doi: 10.1023/A:1024802801048.

[29] I. S. V. Yepes, T. A. Vieira, R. A. B. Suarez, S. R. C. Fernandez, and M. R. R. Gesualdi, "Phase and intensity analysis of non-diffracting beams via digital holography," *Opt. Commun.*, vol. 437, pp. 121–127, Dec. 2018. doi: 10.1016/j.optcom.2018.12.060.

[30] Y. Yang, A. Forbes, and L. Cao, "A review of liquid crystal spatial light modulators: devices and applications," *Opto-Electron. Sci.*, vol. 2, 2023. doi: 10.29026/oes.2023.230026.